nature chemical biology

Chemical genetics reveals a complex functional ground state of neural stem cells

Phedias Diamandis[1–4], Jan Wildenhain[4], Ian D Clarke[1,2], Adrian G Sacher[1,2], Jeremy Graham[1,2], David S Bellows[3], Erick K M Ling[1,2,5], Ryan J Ward[1,2,5], Leanne G Jamieson[1,2,5], Mike Tyers[3,4] & Peter B Dirks[1,2,5,6]

© 2007 Nature Publishing Group http://www.nature.com/naturechemicalbiology

The identification of self-renewing and multipotent neural stem cells (NSCs) in the mammalian brain holds promise for the treatment of neurological diseases and has yielded new insight into brain cancer[1–3]. However, the complete repertoire of signaling pathways that governs the proliferation and self-renewal of NSCs, which we refer to as the 'ground state', remains largely uncharacterized. Although the candidate gene approach has uncovered vital pathways in NSC biology[4–8], so far only a few highly studied pathways have been investigated. Based on the intimate relationship between NSC self-renewal and neurosphere proliferation[8], we undertook a chemical genetic screen for inhibitors of neurosphere proliferation in order to probe the operational circuitry of the NSC. The screen recovered small molecules known to affect neurotransmission pathways previously thought to operate primarily in the mature central nervous system; these compounds also had potent inhibitory effects on cultures enriched for brain cancer stem cells. These results suggest that clinically approved neuromodulators may remodel the mature central nervous system and find application in the treatment of brain cancer.

To profile the signaling network of primary cultures of neural precursor cells (NPCs), we screened 1,267 compounds in the library of pharmacologically active compounds (LOPAC) for inhibitors of neurosphere proliferation, as measured by incorporation of the vital dye thiazolyl blue tetrazolium bromide (MTT) (**Fig. 1a,b** and **Supplementary Table 1** online). A Z′ factor[9] of 0.78 and a Pearson correlation coefficient of 0.981 for replicate screens indicated that the assay was reliable (**Supplementary Methods** online). 160 compounds that significantly inhibited neurosphere proliferation ($P < 0.01$) were clustered into groups of known pharmacologic action (**Table 1** and **Supplementary Table 2** online). Known cytotoxic compounds that target essential cellular processes predictably scored as hits in the screen. Unexpectedly, however, many agents that modulate neurotransmission in the dopamine, serotonin, opioid, glutamate, vanilloid and other pathways potently inhibited growth of NPCs. Many of these agents are used in the clinical treatment of neurological disorders and are traditionally thought to act on mature central nervous system (CNS) cell populations. These compounds induced a variety of neurosphere phenotypes, including changes in sphere number, sphere size, and cell-cell or cell-surface adhesion properties, which suggests that an elaborate balance of these signaling pathways dictates NPC fate (**Fig. 1c**).

To verify hits from the primary screen, 43 representative candidates were retested at the original screen concentration of 3 μM; of these, 40 (93%) showed significant activity ($P<0.05$) (**Supplementary Table 3** online). Because other neural cell types express and signal through a number of neurotransmitter receptors[10], we assessed the selectivity and potency of each agent for a normal mouse astrocyte cell line versus NPCs. Dose-response curves were generated for 28 compounds in both neurosphere and astrocyte cultures and used to determine the effective concentration needed to decrease proliferation by 50% (EC_{50}) (**Fig. 2a–f** and **Supplementary Table 3**). A neurosphere selectivity ratio, defined as $EC_{50(astrocytes)}/EC_{50(neurospheres)}$, was determined for each compound and compared with that of known nonspecific inhibitors of proliferation (**Fig. 2a–c**). Compounds that had a neurosphere selectivity ratio greater than that observed in these control agents (>5.08) were defined as NPC-specific agents (**Fig. 2d–f** and **Table 2**); 12 of the compounds tested showed high selectivity for NPCs. Notably, the serotonin agonist *p*-aminophenethyl-*m*-trifluoromethylphenyl pierazine (PAPP, **14**) and the vanilloid receptor ligand dihydrocapsaicin were respectively 702- and 192-fold more selective for normal NPCs than for astrocyte cultures.

Neurospheres are comprised of a heterogeneous population of NSCs and lineage-restricted progenitor cells. To determine whether the inhibitors affected NSC self-renewal, as opposed to proliferation of more committed precursor populations, we analyzed the higher order colony-forming efficiency of treated neurosphere cultures. With the exception of dihydrocapsaicin, representative compounds from the main neurotransmission classes significantly reduced higher order

[1]The Arthur and Sonia Labatt Brain Tumor Research Centre and [2]Program in Developmental and Stem Cell Biology, The Hospital for Sick Children and University of Toronto, 555 University Avenue, Toronto M5G 1X8, Canada. [3]Samuel Lunenfeld Research Institute, Mount Sinai Hospital, 600 University Avenue, Toronto M5G 1X5, Canada. [4]Department of Medical Genetics and Microbiology, University of Toronto, 1 Kings College Circle, Toronto M5S 1A8, Canada. [5]Department of Laboratory Medicine and Pathobiology, Faculty of Medicine, University of Toronto, Banting Institute, 100 College Street, Toronto M5G 1L5, Canada. [6]Division of Neurosurgery, The Hospital for Sick Children and University of Toronto, 555 University Avenue, Toronto M5G 1X8, Canada. Correspondence should be addressed to M.T. (tyers@mshri.on.ca) or P.B.D. (peter.dirks@sickkids.ca).

Received 14 September 2006; accepted 14 March 2007; published online 8 April 2007; doi:10.1038/nchembio873

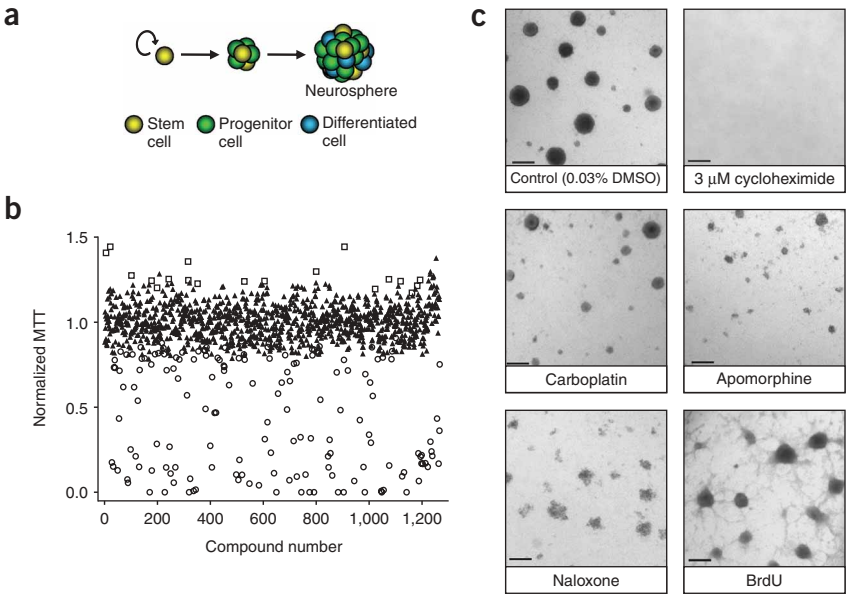

Figure 1 HTS of NPCs. (**a**) Neurospheres are derived from self-renewing multipotent NSCs and contain a heterogeneous mixture of stem cells, progenitor cells, and a very small number of differentiated cells. (**b**) Scatter plot of all 1,267 compounds of the LOPAC library screened against NPCs. 160 compounds (○) were identified as inhibitors of neurosphere proliferation ($P < 0.01$), 19 compounds (□) were identified as activators ($P < 0.01$) and the remaining agents (▲) screened did not have any significant effects on proliferation ($P > 0.01$). (**c**) Examples of phenotypic variation observed in response to particular agents. Scale bars, 250 μm. HTS, high-throughput screen.

neurosphere formation upon re-culture in the absence of drug (**Fig. 2g**). The various inhibitors therefore seem to target the neural precursor pool that is predominantly responsible for sphere formation.

To further delineate the mechanism through which neuromodulatory agents impede expansion of NPCs in culture, we performed time-course analyses for both cell viability and apoptosis. Unlike etoposide (**Fig. 3a**) and cycloheximide (data not shown), which have immediate effects on cell proliferation and viability, the neurotransmission modulators PAPP and ifenprodil decreased viable cell numbers only after 2 d post-treatment (**Fig. 3a**). Similar delayed-onset effects were observed for butaclamol, *p*-fluoro-hexahydrosila-difenidol (*p*-F-HHSiD, **8**) and carbetapentane (data not shown). Consistently, caspase-3 and caspase-7 concentrations were unchanged after 12 h of PAPP and ifenprodil treatment, but increased significantly ($P<0.001$) after 2 d of drug treatment (**Fig. 3b**). This increase in the apoptotic response of treated cells occurred at concentrations of drugs that did not abolish the initial proliferation or viability of these cells (**Fig. 3c**). Finally, expression of the immature NPC marker nestin was substantially decreased after treatment for 2 d with ifenprodil (**Fig. 3d**) and PAPP (data not shown). These results suggest that appropriate neurotransmission signaling is required to maintain NSC proliferation, survival and identity.

As gene expression profiles of brain tumors resemble those of normal and embryonic NPCs[11–14], agents that inhibit normal neural precursor growth may also inhibit cultures of brain tumors that are enriched for cancer stem cells[1,2,11]. We therefore assessed the activity of a subset of NPC-specific inhibitors against low-passage (<4) neurosphere cultures derived from spontaneously formed medulloblastomas in heterozygous patched (*Ptch1*$^{+/-}$) and *Ptch1*$^{+/-}$ *Trp53*$^{-/-}$ mice[15]. Like their normal counterparts, cancerous NPCs from these tumors grow as spheres in serum-free culture and express the neural precursor marker prominin1 (CD133) (**Fig. 4a**,**b**). The NPC-specific agents also potently suppressed the proliferation of both *Ptch1*$^{+/-}$ and *Ptch1*$^{+/-}$ *Trp53*$^{-/-}$ medulloblastoma precursor cell populations (**Fig. 4c** and **Table 2**). Notably, some of these agents were an order of an magnitude more effective in the inhibition of tumor cell growth *in vitro* than the hedgehog signaling inhibitor cyclopamine[16]. The expansion of normal human NPCs and human glioblastoma cells was also inhibited by neuromodulators (**Supplementary Table 4** online). For example, PAPP and ifenprodil had EC_{50} values comparable to those of commonly used nonspecific brain tumor chemotherapeutic drugs, such as carboplatin and etoposide. Re-deployment of well-tolerated pharmacologically active agents may thus afford a new generation of chemotherapeutic agents specific for brain tumor stem cells.

As even well-characterized agents may exert biological effects through off-target pathways[17], we verified that a number of the known receptors for various agents are indeed expressed in both normal and tumor NPCs. The dopamine (DRD2), acetylcholine (M3), NMDA (NR1) and serotonin (5HT-1A) receptors were present in primary and secondary normal mouse neurosphere cultures and *Ptch1*$^{+/-}$ tumor neurosphere cultures, as determined by RT-PCR (**Fig. 4d**). In addition, we were able to use pharmacological inhibitors as a means to assess whether the growth inhibition caused by the dopamine class of neuromodulators depends on transmission through a known receptor.

Table 1 HTS bioactive pharmacological classes

Class[a]	Active agents[b]	Total agents	% active in class
Cytotoxic[c]	38	114	33
Biochemistry	6	46	13
Cannabinoid	1	6	17
Cholinergic	8	77	10
Cyclic nucleotides	4	31	13
Dopamine	22	113	20
Glutamate	9	88	10
Intracellular Ca^{2+}	2	7	29
Ion pump	3	16	19
Lipid	1	9	11
Na^{+} channel	3	17	18
Nitric oxide	5	37	14
Opioid	6	27	22
P2 receptor	2	14	14
Phosphorylation	9	93	10
Serotonin	12	83	14
Vanilloid	2	5	40
Entire screen	160	1,267	13[d]

[a]Includes all classes with a percentage active in class of at least 10%. [b]Only includes inhibitors. [c]Includes antibiotics, apoptosis, cell cycle, cell stress, cytoskeleton and DNA agents. [d]Frequency of whole screen.

© 2007 Nature Publishing Group http://www.nature.com/naturechemicalbiology

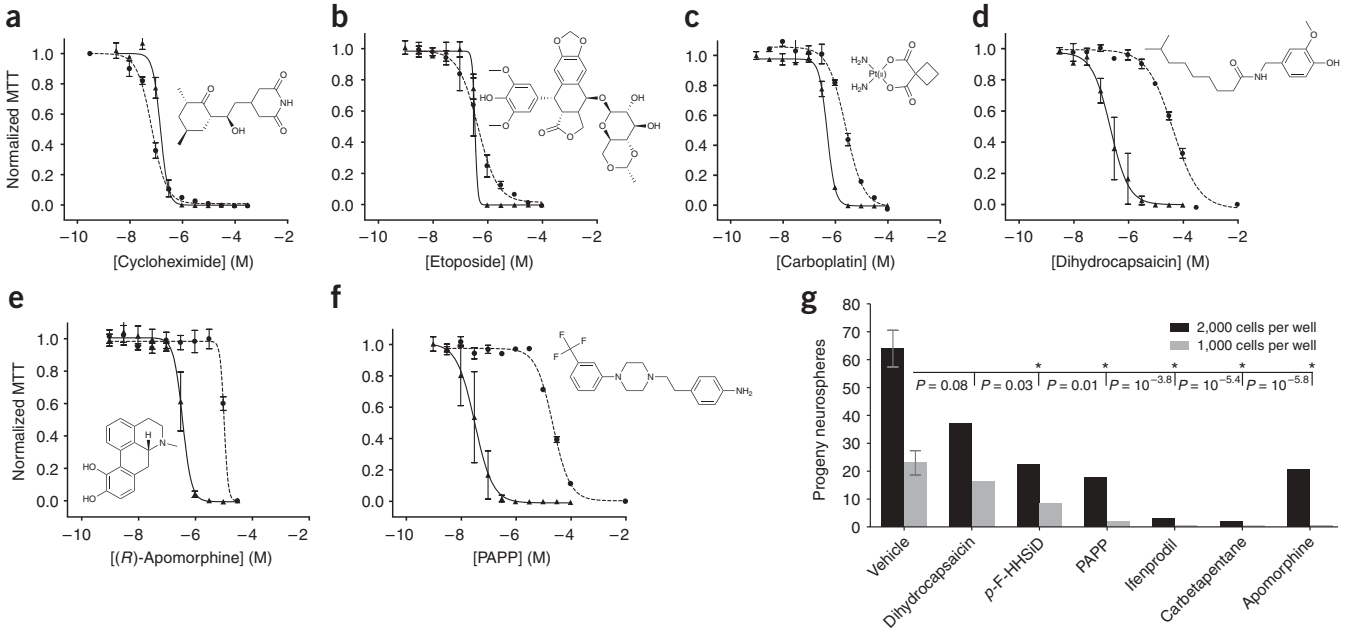

Figure 2 Identification of potent NPC-specific compounds. (**a**–**f**) Dose-response curves and chemical structures of controls: cycloheximide (**a**), etoposide (**b**) and carboplatin (**c**), and of selected newly identified compounds: dihydrocapsaicin (**d**), apomorphine (**e**) and PAPP (**f**). Each plot shows the fitted sigmoidal logistic curve to MTT proliferation assay readings of both astrocytes (- -●- -) and neurosphere cultures (–▲–). Values represent the mean and s.e.m. of three independent experiments. (**g**) Replating colony forming efficiency of pretreated neurosphere cultures. Values represent the number of progeny neurospheres arising from 2,000 or 1,000 cells plated in fresh medium after a 7-d pretreatment of NPCs with the indicated inhibitor at the estimated EC_{75} value. As the EC_{75} of apomorphine did not allow the recovery of sufficient cells, an EC_{50} pretreatment was used for this agent. Sphere counts for vehicle-treated cells represent the mean and s.d. of six separate replicates conducted during two independent experiments. All other values represent the mean of two independent experiments. Asterisks indicate a reproduced statistically significant ($P < 0.05$) reduction in replating efficiency when compared to vehicle control. The larger P value (of the two experiments) is reported. These differences (at both 2,000 and 1,000 cells per well) were confirmed (two-tailed paired t-test) for cultures treated with PAPP ($P_{2,000} = 0.02$; $P_{1,000} = 0.008$) and apomorphine ($P_{2,000} = 0.01$; $P_{1,000} = 0.02$) in three independent trials.

In one example, (±)-sulpride (17), a D2 dopamine receptor antagonist, was able to competitively rescue the inhibitory effects of the D2 and D3 dopamine receptor agonist bromocriptine (18), as judged by both colony formation (**Fig. 4e,f**) and MTT values (data not shown). To further assess the potential for off-target effects of neuromodulators in other classes, we clustered the 160 bioactive agents from the primary screen based on their chemical structures (**Supplementary Table 1**). This analysis demonstrated substantial chemical structural diversity within each of the different neuromodulator classes. For example, the 22 bioactive dopamine agents identified in the screen spanned 10 different structural motif clusters; similarly, the 12 active serotonergic agents covered 10 different chemical clusters (**Supplementary Fig. 1** online). The observed sensitivity of NPCs to these structurally diverse agents is thus likely to arise through effects on known neurotransmission receptors, as opposed to some unknown coincident target.

The *ex vivo* and *in situ* manipulation of NSCs for treating neurological disorders, including brain cancer, will require an understanding of the global signaling network that regulates NSC behavior. Through a chemical genetic approach we have uncovered the existence of a complex functional 'ground state', whereby NSC proliferation and self-renewal is regulated by numerous signaling pathways (**Fig. 4g,h**). Importantly, this cohort includes many neurotransmission pathways previously thought to function only in mature cells of the CNS. Therefore, we infer that NSC proliferation and self-renewal requires an appropriate local environment of neurotransmitter activities, which may be provided by a basal level of autocrine feedback from more committed cells within the neurosphere or even the NSC itself. Indeed, recent studies on individual pathways support the notion that proliferation of different progenitor subpopulations *in vivo* may respond to dopamine, serotonin, acetylcholine and glutamate[18]. Notably, our chemical genetic profile demonstrates the simultaneous operation of these pathways in NPCs cultured under uniform experimental conditions. This sensitivity of NPC cultures to a spectrum of neuroactive compounds also supports the notion of lineage priming in the NSC compartment, similar to that seen in hematopoietic stem cells[19].

Though we have yet to definitively identify the precursor subpopulations targeted by each inhibitor identified in the screen, the strong selectivity of many agents for NPCs and primary brain tumor cells suggests that the affected pathways lie high in the hierarchical organization of the neuronal lineage. Indeed, the often complete inhibition of neurosphere proliferation and the effects on secondary replating suggest that stem cells and/or very early progenitor components of the population are affected by these agents. The finding that both inhibitors and activators of specific pathways inhibit neurosphere proliferation (for example, dopamine receptor agonists and antagonists) suggests that a complex signaling landscape dictates NSC fate[20]. We note that the pro-proliferative culture conditions used in the neurosphere assay may have biased the assay against identification of significant numbers of small molecules that stimulate proliferation. A small-molecule activator of embryonic stem cell proliferation has recently been identified[21], which suggests that analogous screens may succeed in identifying activators of NPC proliferation.

© 2007 Nature Publishing Group http://www.nature.com/naturechemicalbiology

Table 2 Highly potent and highly selective compounds identified by HTS of neurospheres

Name	Action	Target	Selectivity	Neurosphere EC_{50} (μM)	Astrocyte EC_{50} (μM)	Neurosphere selectivity	*Ptch1*$^{+/-}$ neurosphere EC_{50} (μM)[b]	*Ptch1*$^{+/-}$ *Trp53*$^{-/-}$ neurosphere EC_{50} (μM)[b]
Controls								
Cycloheximide (1)	Inhibitor	Protein synthesis	60S ribosome	0.142	0.071	0.50	0.042	0.054
Etoposide (2)	Inhibitor	Topoisomerase	Topo II	0.340	0.433	1.28	0.208	n.t.
Carboplatin (3)	Intercalator	DNA	n.a.	0.489	2.453	5.08	0.196	n.t.
Selected hits[a]								
(±) Butaclamol (4)	Antagonist	Dopamine receptor	D2 > D1	0.785	12.34	15.7	0.751	2.533
(*R*)-(–)-Propylnorapomorphine (5)	Agonist	Dopamine receptor	D2	0.351	8.230	23.4	0.199	n.t.
(*R*)-(–)-Apomorphine (6)	Agonist	Dopamine receptor	n.a.	0.350	10.19	29.1	0.168	0.683
cis-(*Z*)-Flupenthixol (7)	Antagonist	Dopamine receptor	n.a.	0.199	1.182	5.93	0.187	n.t.
p-F-HHSiD (8)	Antagonist	Acetylcholine receptor	M3 > M1 > M2	0.441	5.815	13.2	1.125	1.373
Ifenprodil (9)	Antagonist	NMDA receptor	Polyamine site	0.616	11.06	17.9	0.451	0.807
Carbetapentane (10)	Agonist	Opioid receptor	Sigma 1	0.756	28.16	37.3	2.083	2.040
Fenretinide (11)	Agonist	Retinoic acid receptor	n.a.	0.334	2.399	7.18	0.204	n.t.
WHI-P131 (12)	Antagonist	JAK3	n.a.	2.346	n.d.	>10	1.525	n.t.
SB 202190 (13)	Antagonist	p38 MAPK	n.a.	8.063	64.8	8.04	3.006	n.t.
PAPP (14)	Agonist	Serotonin receptor	5-HT1A	0.031	21.82	702	0.169	0.097
Dihydrocapsaicin (15)	Agonist	Vanilloid receptor	VR1	0.218	41.83	192	0.020	0.651
Cyclopamine (16)	Antagonist	Smoothened		n.t.	n.t.	n.a.	1.00	13.44

[a]Compounds listed represent confirmed hits with high selectivity for NPCs (neurosphere selectivity >5). [b]*Ptch1*$^{+/-}$ *and Ptch1*$^{+/-}$ *Trp53*$^{-/-}$ neurosphere cultures were derived from mouse cerebellar tumor samples. n.a., not applicable; n.d., not determined at highest tested dose (30 μM); n.t., not tested.

The unanticipated actions of well-characterized clinical agents on NPCs may account in whole or in part for the observed clinical benefits of these agents and/or the adverse side effects that arise after prolonged therapy. Effective *in vivo* concentrations of the anti-Parkinsonian drug apomorphine reach 6–7 μM[22], which is substantially higher than doses that affect NPCs *in vitro*. Thus the regulation of NSC proliferation by neurotransmitters may also dictate how the CNS is wired both during development and in the adult brain[23]. Recent evidence suggests that appropriate GABA stimulation of NPCs is required for the proper integration of neurons in the adult hippocampus[24]. Through structure-activity analysis, we also identified specific chemical substitutions that are important for the bioactivity of these agents in our *in vitro* system (**Supplementary Figs. 2** and **3** online). Such modifications to the core chemical structure of many clinically used agents may afford a way to regulate the potentially therapeutic or harmful effects these drugs have on NPCs.

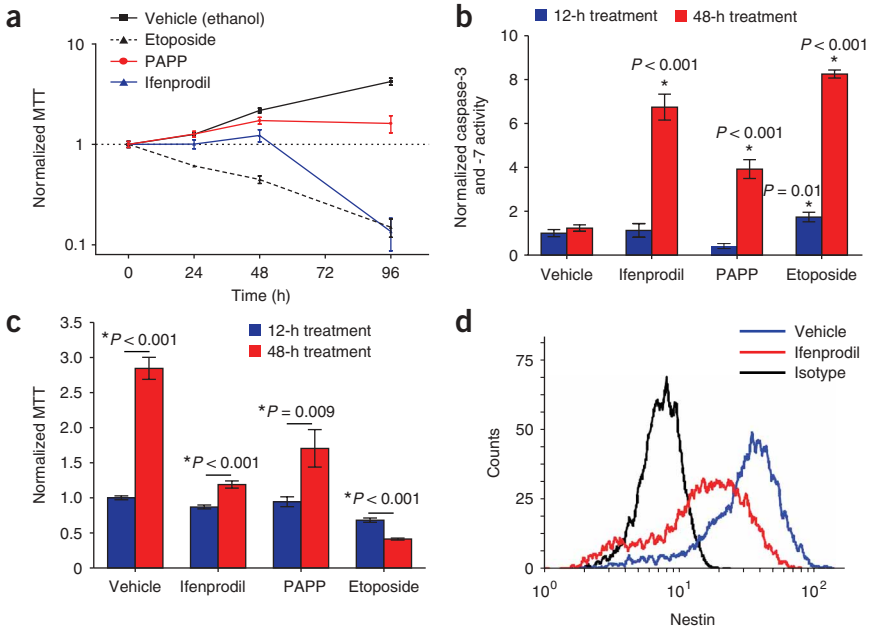

Figure 3 Temporal effects of neuromodulators on NPC viability and apoptotic response. (**a**) Proliferation dynamics of PAPP-, ifenprodil- and etoposide-treated NPCs. (**b**) Normalized caspase-3 and caspase-7 activity in NPCs after 12 h and 48 h of drug treatment. Asterisk indicates a significant change (two-tailed *t*-test) from the corresponding vehicle-treated data point. (**c**) Corresponding MTT values taken at 12 h and 2 d for the caspase-3 and caspase-7 experiments shown in **b**. All values represent the mean and s.d. of one representative experiment (from three independent trials) of NPCs treated with PAPP (1 μM), ifenprodil (3 μM), etoposide (3 μM) or vehicle. (**d**) Flow cytometric analysis of the neural precursor marker nestin in NPCs after 2 d of treatment with ifenprodil (5 μM) or vehicle. Representative histograms of vehicle-treated (20% nestin negative) and ifenprodil-treated (63% nestin negative) cells compared with the isotype control (100% nestin negative) are shown from two independent experiments.

© 2007 Nature Publishing Group http://www.nature.com/naturechemicalbiology

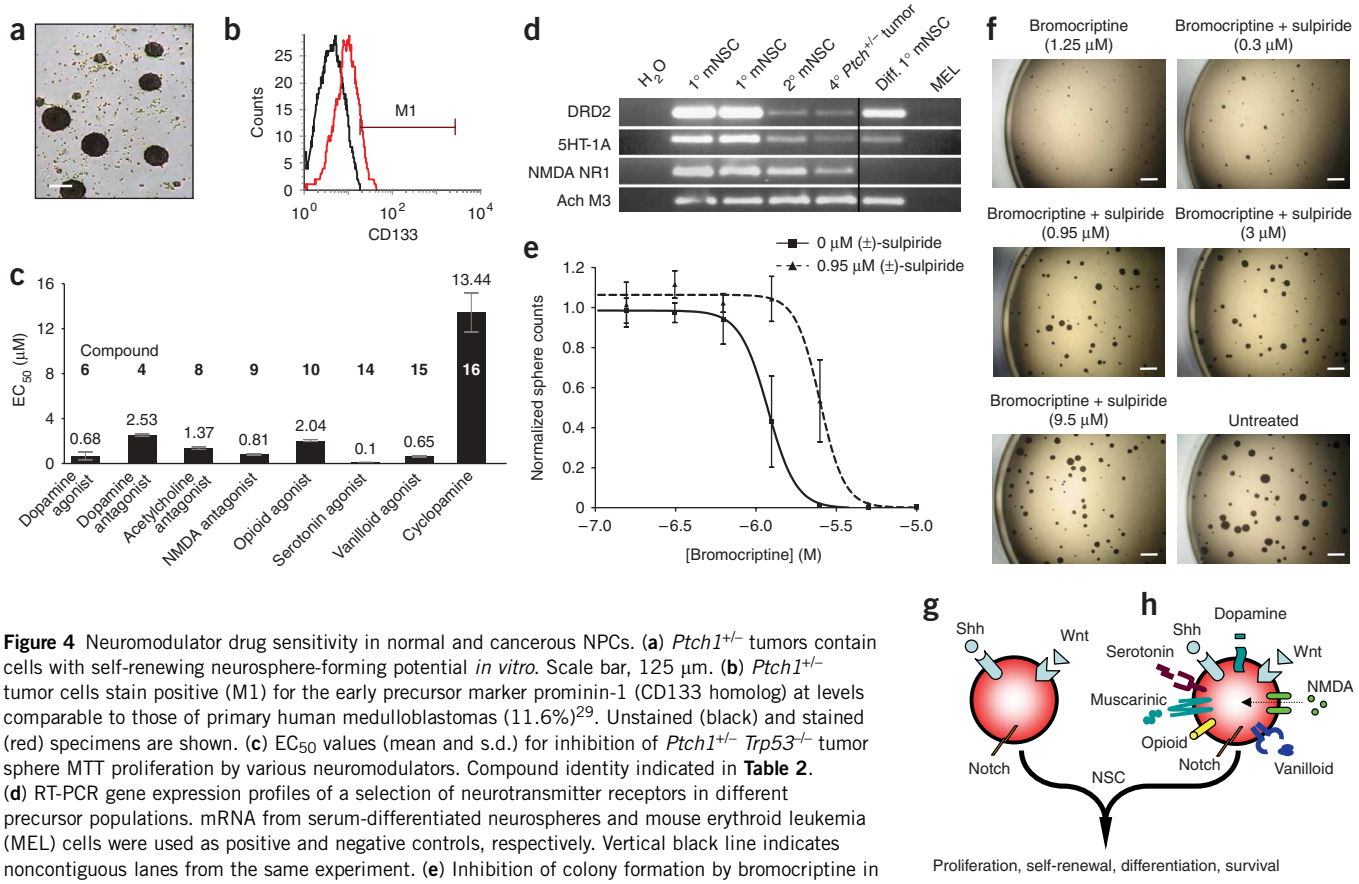

Figure 4 Neuromodulator drug sensitivity in normal and cancerous NPCs. (**a**) *Ptch1*$^{+/-}$ tumors contain cells with self-renewing neurosphere-forming potential *in vitro*. Scale bar, 125 μm. (**b**) *Ptch1*$^{+/-}$ tumor cells stain positive (M1) for the early precursor marker prominin-1 (CD133 homolog) at levels comparable to those of primary human medulloblastomas (11.6%)[29]. Unstained (black) and stained (red) specimens are shown. (**c**) EC_{50} values (mean and s.d.) for inhibition of *Ptch1*$^{+/-}$ *Trp53*$^{-/-}$ tumor sphere MTT proliferation by various neuromodulators. Compound identity indicated in **Table 2**. (**d**) RT-PCR gene expression profiles of a selection of neurotransmitter receptors in different precursor populations. mRNA from serum-differentiated neurospheres and mouse erythroid leukemia (MEL) cells were used as positive and negative controls, respectively. Vertical black line indicates noncontiguous lanes from the same experiment. (**e**) Inhibition of colony formation by bromocriptine in cultures with and without (±)-sulpiride supplementation. Normalized mean and s.e.m. values of three independent triplicate cultures are shown. Sulpiride challenge significantly shifted the EC_{50} of bromocriptine from 1.2 μM (without sulpiride) to 2.5 μM (with sulpiride) ($P < 0.05$), thereby indicating a rescue effect. (**f**) Representative micrographs of the inhibitory effects of bromocriptine on NPC expansion when challenged with a competitive antagonist. Scale bars, 500 μm. (**g**,**h**) Functional ground state of NSCs: current models of the NSC hierarchy focus on developmental signaling pathways such as Wnt, Notch and Sonic Hedgehog (**g**); compounds identified in the HTS approach reveal that the NSC ground state and cell fate decision-making depend on a complex circuitry that includes many neurotransmission signaling pathways (**h**).

In light of the evidence that CNS tumors are maintained by cancer stem cells[1,3], which have similarities to normal NSCs[11], the potent and selective antiproliferative agents identified in this study may presage a new generation of therapeutic agents in brain cancer, although further *in vivo* testing is required[3]. Notably, a retrospective analysis of cancer incidence in individuals with Parkinson disease revealed a significant reduction in the incidence of brain tumors relative to the expected incidence in the general population[25]; this correlation may derive from the effect of anti-Parkinsonian drugs on the NPCs from which brain tumors are thought to arise. As the complex NSC ground state we propose is likely to at least in part define the identity of brain tumor stem cells, re-deployment of pharmacologically approved neuroactive agents may provide an immediate and nontoxic means to treat often intractable CNS tumors.

METHODS

Primary embryonic mouse NSC isolation and culture. Isolation and culture of primary embryonic (e14.5) mouse NSCs was performed as previously described in chemically defined NSC medium[26] containing 20 ng ml^{-1} human recombinant epidermal growth factor (Sigma), 20 ng ml^{-1} basic fibroblast growth factor (Upstate) and 2 μg ml^{-1} heparin (Sigma). Cells were fed every 2–3 d[27].

Secondary mouse NSC neurosphere culture and chemical screens. Before chemical screens and other manipulations, the NSC fraction in culture was expanded by growing freshly dissected cells as primary neurospheres[28] in bulk culture (10^6 cells ml^{-1}). After 7 d, primary neurospheres were collected and enzymatically digested for 3 min at 37 °C using Accutase (Sigma), mechanically dissociated with a 1-ml pipette and passed through a cell strainer (Falcon). Viable cells were plated at low cell densities (20 cells μl^{-1}) in 96-well plates (Falcon) in a final volume of 100 μl and screened in singlets against the LOPAC library (Sigma) at a concentration of 3 μM (0.03% DMSO). On day 4, each well in the screen was supplemented with an additional 50 μl of fresh mouse NSC medium and another aliquot of the LOPAC library (maintaining the final concentration of each compound at 3 μM). Secondary neurosphere cultures were then incubated for an additional 3 d (until day 7), at which point the effect of each compound was assessed by quantifying the total proliferation of each well using the incorporation of the vital dye MTT (Sigma) as previously described[29].

Statistical analysis for chemical screen. Background plate effects (**Supplementary Methods**) occurring from the evaporation of medium over the course of the experiment were estimated by:

$$b_i = \frac{1}{N - N_i^h} \sum_{j=1}^{N} x'_{i,j}$$

where $x'_{i,j}$ is the value at well i of plate j, N_i^h is the number of excluded hits or outliers that were 2 s.d. below the mean, N is the total number of plates in the screen, and b_i is the estimated background at each well position[30]. The

© 2007 Nature Publishing Group http://www.nature.com/naturechemicalbiology

respective background was then subtracted from the raw MTT value measured for each point (**Supplementary Methods**). To calculate significance (z score and P value), the theoretical probability density function $N(1.0, 0.11)$ was fitted to the empirical normalized distribution obtained from the screen (**Supplementary Methods**). Compounds that caused optical density readings to significantly deviate from this predicted underlying distribution function ($P < 0.01$) were designated as bioactive[31].

Dose-response curves and EC_{50} calculations. Potency of confirmed bioactive compounds was quantified by generating dose-response curves for mouse NSC under the same cell density and culture conditions described for the initial screen. Starting from initial concentrations between 300 and 30 μM, each compound was titrated across a series of ten half-log dilutions. Each agent was tested in triplicate in at least three independent experiments. EC_{50} values for each agent were calculated by fitting the data points to the four-parameter logistic sigmoidal dose-response curve:

$$Y = \mathrm{EC}_{100} + \frac{\mathrm{EC}_0 - \mathrm{EC}_{100}}{1 + 10^{\log(\mathrm{EC}_{50} - X)(\mathrm{HillSlope})}}$$

where X is the logarithm of concentration and Y is the predicted response. Curve fitting was performed with GraphPad Prism software (GraphPad Software, Inc.).

Note: Supplementary information and chemical compound information is available on the Nature Chemical Biology website.

ACKNOWLEDGMENTS

We thank L. Lee, P. Northcode and S. Dolma for technical expertise, G. Giaever and C. Nislow for access to cheminformatics software, and S. Cordes for critical suggestions regarding pharmacological rescue experiments. P.D. is supported by a Canadian Institutes of Health Research (CIHR) MD/PhD studentship. P.B.D. is supported by grants from the National Cancer Institute of Canada, with funds from the Canadian Cancer Society, CIHR and the Stem Cell Network, and from donations from BrainChild and the Durigon (Jessica's Footprint), Baker, Blyth and Kolic families. M.T. is supported by grants from the CIHR and a Canada Research Chair in Bioinformatics and Functional Genomics.

COMPETING INTERESTS STATEMENT

The authors declare no competing financial interests.

Published online at http://www.nature.com/naturechemicalbiology
Reprints and permissions information is available online at http://npg.nature.com/reprintsandpermissions

1. Galli, R. *et al.* Isolation and characterization of tumorigenic, stem-like neural precursors from human glioblastoma. *Cancer Res.* **64**, 7011–7021 (2004).
2. Hemmati, H.D. *et al.* Cancerous stem cells can arise from pediatric brain tumors. *Proc. Natl. Acad. Sci. USA* **100**, 15178–15183 (2003).
3. Singh, S.K. *et al.* Identification of human brain tumour initiating cells. *Nature* **432**, 396–401 (2004).
4. Ahn, S. & Joyner, A.L. *In vivo* analysis of quiescent adult neural stem cells responding to Sonic hedgehog. *Nature* **437**, 894–897 (2005).
5. Groszer, M. *et al.* PTEN negatively regulates neural stem cell self-renewal by modulating G0–G1 cell cycle entry. *Proc. Natl. Acad. Sci. USA* **103**, 111–116 (2006).
6. Hitoshi, S. *et al.* Notch pathway molecules are essential for the maintenance, but not the generation, of mammalian neural stem cells. *Genes Dev.* **16**, 846–858 (2002).
7. Lie, D.C. *et al.* Wnt signalling regulates adult hippocampal neurogenesis. *Nature* **437**, 1370–1375 (2005).
8. Molofsky, A.V. *et al.* Bmi-1 dependence distinguishes neural stem cell self-renewal from progenitor proliferation. *Nature* **425**, 962–967 (2003).
9. Zhang, J.H., Chung, T.D. & Oldenburg, K.R. A simple statistical parameter for use in evaluation and validation of high throughput screening assays. *J. Biomol. Screen.* **4**, 67–73 (1999).
10. Seifert, G., Schilling, K. & Steinhauser, C. Astrocyte dysfunction in neurological disorders: a molecular perspective. *Nat. Rev. Neurosci.* **7**, 194–206 (2006).
11. Lee, J. *et al.* Tumor stem cells derived from glioblastomas cultured in bFGF and EGF more closely mirror the phenotype and genotype of primary tumors than do serum-cultured cell lines. *Cancer Cell* **9**, 391–403 (2006).
12. Phillips, H.S. *et al.* Molecular subclasses of high-grade glioma predict prognosis, delineate a pattern of disease progression, and resemble stages in neurogenesis. *Cancer Cell* **9**, 157–173 (2006).
13. Taylor, M.D. *et al.* Radial glia cells are candidate stem cells of ependymoma. *Cancer Cell* **8**, 323–335 (2005).
14. Pomeroy, S.L. *et al.* Prediction of central nervous system embryonal tumour outcome based on gene expression. *Nature* **415**, 436–442 (2002).
15. Corcoran, R.B. & Scott, M.P. A mouse model for medulloblastoma and basal cell nevus syndrome. *J. Neurooncol.* **53**, 307–318 (2001).
16. Berman, D.M. *et al.* Medulloblastoma growth inhibition by hedgehog pathway blockade. *Science* **297**, 1559–1561 (2002).
17. Macdonald, M.L. *et al.* Identifying off-target effects and hidden phenotypes of drugs in human cells. *Nat. Chem. Biol.* **2**, 329–337 (2006).
18. Hagg, T. Molecular regulation of adult CNS neurogenesis: an integrated view. *Trends Neurosci.* **28**, 589–595 (2005).
19. Enver, T. & Greaves, M. Loops, lineage, and leukemia. *Cell* **94**, 9–12 (1998).
20. Sharom, J.R., Bellows, D.S. & Tyers, M. From large networks to small molecules. *Curr. Opin. Chem. Biol.* **8**, 81–90 (2004).
21. Chen, S. *et al.* Self-renewal of embryonic stem cells by a small molecule. *Proc. Natl. Acad. Sci. USA* **103**, 17266–17271 (2006).
22. Butterworth, R.F. & Barbeau, A. Apomorphine: sterotyped behavior and regional distribution in rat brain. *Can. J. Biochem.* **53**, 308–311 (1975).
23. Lledo, P.M., Alonso, M. & Grubb, M.S. Adult neurogenesis and functional plasticity in neuronal circuits. *Nat. Rev. Neurosci.* **7**, 179–193 (2006).
24. Ge, S., Pradhan, D.A., Ming, G.L. & Song, H. GABA sets the tempo for activity-dependent adult neurogenesis. *Trends Neurosci.* **30**, 1–8 (2007).
25. Lalonde, F.M. & Myslobodsky, M. Are dopamine antagonists a risk factor for breast cancer? An answer from Parkinson's disease. *Breast* **12**, 280–282 (2003).
26. Uchida, N. *et al.* Direct isolation of human central nervous system stem cells. *Proc. Natl. Acad. Sci. USA* **97**, 14720–14725 (2000).
27. Tropepe, V. *et al.* Distinct neural stem cells proliferate in response to EGF and FGF in the developing mouse telencephalon. *Dev. Biol.* **208**, 166–188 (1999).
28. Gritti, A. *et al.* Epidermal and fibroblast growth factors behave as mitogenic regulators for a single multipotent stem cell-like population from the subventricular region of the adult mouse forebrain. *J. Neurosci.* **19**, 3287–3297 (1999).
29. Singh, S.K. *et al.* Identification of a cancer stem cell in human brain tumors. *Cancer Res.* **63**, 5821–5828 (2003).
30. Kevorkov, D. & Makarenkov, V. Statistical analysis of systematic errors in high-throughput screening. *J. Biomol. Screen.* **10**, 557–567 (2005).
31. Chambers, J.M., Cleveland, W.S., Kleiner, B. & Tukey, P.A. *Graphical Methods for Data Analysis* (Chapman and Hall, New York, 1983).

© 2007 Nature Publishing Group http://www.nature.com/naturechemicalbiology